ELectronics EXpress

IEICE Electronics Express, Vol.8, No.21, 1757–1762

Meshless physical simulation of semiconductor devices using a wavelet-based nodes generator

Rashid Mirzavand[1], **Abdolali Abdipour**[1a)], **Gholamreza Moradi**[1], **and Masoud Movahhedi**[2]

[1] *Microwave/mm-wave & Wireless Communication Research Lab, Electrical Engineering Department, Amirkabir University of Technology, Tehran, 15914, Iran*

[2] *Electrical Engineering Department, Shahid Bahonar University of Kerman, Kerman, Iran*

a) *abdipour@aut.ac.ir*

Abstract: This paper describes a meshless method with wavelet-based nodes for the two-dimensional time-dependent simulation of semiconductor devices. In this method the solution is approximated using global radial basis functions (RBF) and distributed wavelet-generated points. This allows the computation of problems with complex-shaped boundaries and forming fine and coarse points abundance in locations where variable solutions change rapidly and slowly, respectively. The method is suitable for the semiconductor part of very time consuming global modeling of microwave/millimeter wave circuits due to a large reduction of number of nodes with an acceptable results.

Keywords: semiconductor devices, meshless, wavelet

Classification: Electron devices, circuits, and systems

References

[1] M. Zerroukat, H. Power, and C. S. Chen, "A numerical method for heat transfer problems using collocation and radial basis functions," *Int. J. Numer. Meth. Eng.*, vol. 42, no. 7, pp. 1263–1278, 1998.

[2] J. Li, A. H.-D. Cheng, and C. S. Chen, "A comparison of efficiency and error convergence of multiquadric collocation method and finite element method," *Eng. Anal. Bound. Elem.*, vol. 27, no. 3, pp. 251–257, 2003.

[3] L. Jameson, "Wavelet-based grid generation," *ICASE Report*, no. 96-31, NASA Langley Research Center, Hampton, 1996.

[4] T. Grasser, T. W. Tang, H. Kosina, and S. Selberherr, "A review of hydrodynamic and energy-transport models for semiconductor device simulation," *Proc. IEEE*, vol. 91, pp. 251–274, 2003.

[5] Z. M. Wu, "Compactly supported positive definite radial functions," *Adv. Comput. Math.*, vol. 4, pp. 283–292, 1995.

DOI: 10.1587/elex.8.1757
Received December 16, 2010
Accepted September 27, 2011
Published November 10, 2011

1 Introduction

Many different approaches to the simulation of semiconductor devices have been developed in the past. All of these techniques are fundamentally dependent upon the solution of the Poisson equation along with the basic carrier transport equations. In this paper, the semiconductor analysis is based on the time-domain drift-diffusion model (DDM). The set of DDM equations contains the Poisson equation and the carrier transport equations, obtained by splitting the Boltzmann transport equation (BTE) into its first two moments. The DDM assumes that the carrier velocity is dependent on the electric field only. In comparison to other, more rigorous techniques for numerical modeling of semiconductor devices, the DDM is a relatively simple technique with better convergence of the algorithm and shorter computational times. Therefore, it is more suitable for use by a design engineer. Recently, considerable effort has been devoted to the development of meshless methods to find the numeric solution of partial differential equations [1]. This method has shown to be more efficient than the traditional Finite Difference and Finite Element Methods [2]. A meshless method does not require any connectivity information, but only requires nodes to generate shape functions. Usually, the nodes are generated randomly. But in a semiconductor device simulation random points are not appropriate because of large difference between substrate and doped region sizes. Wavelets provide the scales of information at every location which is needed for effective grid generation. This paper presents a numerical method to solve the DDM equation by approximating directly the solution using global radial basis functions. The nodes will be provided by the wavelet based grid generation algorithm explained in [3]. The method is similar to finite differences but with the advantage of arbitrary point locations.

2 Transistor physical model based on RBF

An approximation of a function $u(x)$ may be written as a linear combination of N radial basis functions as,

$$u^h(\mathbf{x}) \simeq \sum_{i=1}^{N} \phi_i(\mathbf{x}) a_i = \Phi^T(\mathbf{x})\mathbf{a} \; ; \;\; \mathbf{x} \in R^d \tag{1}$$

where N is the number of data points, $\mathbf{x} = (x^1, \; x^2, \; \ldots, \; x^d)$ is the position vector, d is the dimension of the problem, a_i's are coefficients to be determined, $\phi_i(\mathbf{x}) = \phi(\mathbf{x}, \mathbf{x}_i)$ is the radial basis function, and $\Phi(\mathbf{x}) = [\phi_1(\mathbf{x}), \phi_2(\mathbf{x}), \ldots, \phi_N(\mathbf{x})]$. Defining $\mathbf{P}(\mathbf{x}) = \Phi^T(\mathbf{x})\mathbf{A}^{-1}$, the coefficients a_i are determined by forcing the interpolation to pass through all the N collocation points $\{\mathbf{x}_1, \mathbf{x}_2, \ldots, \mathbf{x}_N\}$, resulting in

$$u^h(\mathbf{x}) = \mathbf{P}(\mathbf{x})\mathcal{U} \tag{2}$$

DOI: 10.1587/elex.8.1757
Received December 16, 2010
Accepted September 27, 2011
Published November 10, 2011

where $\mathcal{U} = [u(\mathbf{x}_1), u(\mathbf{x}_2), \ldots, u(\mathbf{x}_N)]^T$ and

$$\mathbf{A} = \begin{bmatrix} \Phi(\mathbf{x}_1) \\ \Phi(\mathbf{x}_2) \\ \vdots \\ \Phi(\mathbf{x}_N) \end{bmatrix} = \begin{bmatrix} \phi_1(\mathbf{x}_1) & \phi_2(\mathbf{x}_1) & \cdots & \phi_N(\mathbf{x}_1) \\ \phi_1(\mathbf{x}_2) & \phi_2(\mathbf{x}_2) & \cdots & \phi_N(\mathbf{x}_2) \\ \vdots & \vdots & \ddots & \vdots \\ \phi_1(\mathbf{x}_N) & \phi_2(\mathbf{x}_N) & \cdots & \phi_N(\mathbf{x}_N) \end{bmatrix} \tag{3}$$

The first-order partial derivative of function, respect to the space variables, can be expressed as

$$\frac{\partial u^h(\mathbf{x})}{\partial \mathcal{X}} = \mathbf{P}_{,\mathcal{X}}(\mathbf{x})\mathcal{U} \;\; ; \;\; \mathcal{X} \in \{x^1,\ x^2,\ \ldots,\ x^d\} \tag{4}$$

where

$$\mathbf{P}_{,\mathcal{X}}(\mathbf{x}) = \Phi^T_{,\mathcal{X}}(\mathbf{x})A^{-1} = [\phi_{1,\mathcal{X}}(\mathbf{x}), \phi_{2,\mathcal{X}}(\mathbf{x}), \ldots, \phi_{N,\mathcal{X}}(\mathbf{x})]^T A^{-1} \tag{5}$$

and $\phi_{j,\mathcal{X}}(\mathbf{x}) = \partial\phi_j(\mathbf{x})/\partial\mathcal{X}$. The second-order partial derivative of function is defined similarly using $\mathbf{P}_{,\mathcal{X}\mathcal{X}} = \Phi^T_{,\mathcal{X}\mathcal{X}}A^{-1}$.

In this paper we simulate a microwave/mm-wave transistor MESFET which is a unipolar device. For this device, the DDM equations to be solved are as follows [4],

$$\vec{J}_n = qn\mu_n(\vec{E}, N_d^+)\vec{E} + qD_n(\vec{E}, N_d^+)\nabla n \tag{6}$$

$$\frac{\partial n}{\partial t} = \frac{1}{q}\nabla \cdot \vec{J}_n \tag{7}$$

$$\nabla^2\varphi = -\frac{q}{\varepsilon_0\varepsilon_r}(N_d^+ - n) \tag{8}$$

where φ is the potential, $\vec{E} = -\nabla\phi$, N_d^+ is the doping profile, n is the electron (carrier) density, μ_n is the mobility coefficient and $D_n = \mu_n K_B T/q$.

According to Eq. (4), the approximation of all components in the Eqs. (6)–(8) can be expanded with the same RBF for $d = 2$ and $\mathbf{x} = (x,\ y)$ as,

$$n(\mathbf{x}, t) = \mathbf{P}\mathcal{N}(t) \tag{9}$$

$$\varphi(\mathbf{x}, t) = \mathbf{P}\mathcal{P}(t) \tag{10}$$

$$J_x(\mathbf{x}, t) = \mathbf{P}\mathcal{J}_x(t),\ J_y(\mathbf{x}, t) = \mathbf{P}\mathcal{J}_y(t) \tag{11}$$

$$E_x(x, t) = \mathbf{P}\mathcal{E}_x(t),\ E_y(\mathbf{x}, t) = \mathbf{P}\mathcal{E}_y(t) \tag{12}$$

where $\mathcal{N}(t)$, $\mathcal{P}(t)$, $\mathcal{J}_x(t)$, $\mathcal{J}_y(t)$, $\mathcal{E}_x(t)$ and $\mathcal{E}_y(t)$ are unknown time coefficient vectors to be computed at the collocation nodes. Thus, Eqs. (6)–(8) discretize using Eqs. (9)–(12) and the finite difference approximation for the time derivative as,

$$\mathcal{N}^{k+1} = \mathbf{P}^{-1}\mathbf{P}\mathcal{N}^k + \mathbf{P}^{-1}(\mathbf{P}_{,x}\mathcal{J}_x^k + \mathbf{P}_{,y}\mathcal{J}_y^k)/q \tag{13}$$

$$\mathcal{J}_x^{k+1} = -qn\mu\mathbf{P}^{-1}\mathbf{P}_{,x}\mathcal{P}^k + qD_n\mathbf{P}^{-1}\mathbf{P}_{,x}\mathcal{N}^k \tag{14}$$

$$\mathcal{J}_y^{k+1} = -qn\mu\mathbf{P}^{-1}\mathbf{P}_{,y}\mathcal{P}^k + qD_n\mathbf{P}^{-1}\mathbf{P}_{,y}\mathcal{N}^k \tag{15}$$

$$\mathcal{P}^{k+1} = -q(\mathbf{P}_{,xx} + \mathbf{P}_{,yy})^{-1}(N_d^+ - \mathbf{P}\mathcal{N}^k)/\varepsilon \tag{16}$$

The computations of unknowns are simple and straightforward operations from Eqs. (13)–(16). Furthermore, if the same collocation points and a constant time-stepping scheme are used throughout the computational process,

DOI: 10.1587/elex.8.1757
Received December 16, 2010
Accepted September 27, 2011
Published November 10, 2011

$\mathbf{P}^{-1}$ computed only once, hence the right-hand-side of Eqs. (13)–(16) are simple operations of $O(N)$.

Similar to the finite differences, Eq. (14) is conditionally stable. However, the stability of the scheme can easily be preserved by an automatic and progressively discarded time sub-divisions as suggested in [1].

After calculating the distributions of potential and carrier density, we can determine where quantities vary rapidly and slowly. In domains that the variation of parameters is high, node generator subprogram add more nodes to initial uniform mesh. By this method, we can generate a nonuniform mesh that is dense in momentous places.

3 Mesh generation using wavelet scheme

The *DC* simulation is started with the evenly-spaced grid points. This grid is used to calculate $\mathbf{P}$ for first time step. After solving Eqs. (13)–(16) for this time step, we use the interpolating wavelet scheme and obtain a sparse point representation for solving equations for the second time step. The magnitude of wavelet coefficients choose which grid points to use [3] in the following manner for a semiconductor simulation. First, a threshold on the wavelet coefficients of carrier density is applied to the longitudinal cross section of the structure to remove some grid points. Then, it is applied to the transverse cross section of carrier density. These two grids are combined by logical 'AND' in order to obtain an overall grid by applying wavelet scheme to carrier density. The proposed scheme removes grid points where variable solutions change slowly and maintain grid points where their change rapidly. Similar operations are used to achieve a sparse grid from the potential distribution. Because the variation of potential is slow, therefore the number of potential mesh nodes is smaller than the number of carrier density mesh nodes. Final grid is obtained from logical 'OR' combination of the generated grids from potential and carrier densities. Using this nodes, Eqs. (13)–(16) are solved and then next step sparse points are obtained by applying wavelet scheme to the results. This process is continued until reaching the maximum desired ratio between the maximum and the minimum values of Δx and Δy or reaching the steady-state *DC* solution. Because the *DC* solution is used in the *AC* analysis as the initial values and also the level of *AC* excitation is lower than the *DC* level at most times, therefore one can conclude after applying the *AC* excitation to the structure, the distributions of parameters will fix approximately. For this reason, we can use the nonuniform mesh generated from the *DC* solution in the *AC* analysis.

4 Simulation results

Several choices are possible as radial basis $\phi(\mathbf{x}, \mathbf{x}_i)$, e.g. multiquadratics or spline functions. In this paper, the compactly supported RBF proposed by Wu [5] is used as,

$$\phi(x, x_i) = \phi(r_i) = \begin{cases} (1-r_i)^4(4+16r_i+12r_i^2+3r_i^3) & r_i \le 1 \\ 0 & \text{others} \end{cases} \quad (17)$$

DOI: 10.1587/elex.8.1757
Received December 16, 2010
Accepted September 27, 2011
Published November 10, 2011

where $r_i = \|\mathbf{x} - \mathbf{x}_i\| / d_{mi}$. Here, d_{mi} represents the supported domain radius at the collocation nodes $\mathbf{x}_i$,

$$d_{mi} = d_{\max} C_i \tag{18}$$

where $d_{\max}$ is a scaling parameter and C_i at a particular node is determined by searching for enough neighbor nodes such that A in Eq. (3) becomes non singular. The use of a compactly supported version of the RBF kernel result in a sparse matrix, and thus decrease the computational cost and memory requirements. The transistor considered in this simulation is a $0.3\,\mu$m gate MESFET. Fig. 1 presents the conventional $2D$ structure used in our simulation. The simulation is started by a uniform mesh that covers the $2D$ cross section of the MESFET with $\{(140-1)\times(33-1)\}$ internal and $\{2\times140\times33\}$ boundary points. The device is biased to $V_{ds} = 3\,\mathrm{V}$ and $V_{gs} = -0.5\,\mathrm{V}$. In a trade off between the simulation time and the solution accuracy, the threshold value in wavelet scheme has been set to 0.00008 for normalized quantities. Therefore, the final non-uniform grid has 1219 internal and 115 boundary points, that shows about 72% compression from uniform mesh. The state of the MESFET under DC steady state is represented by the distribution of potential and carrier density. Fig. 2 shows the potential and normalized carrier density (n/N_{DI}) distributions obtained by the conventional uniform FDTD method, Meshfree method with the uniform distributed nodes, and Meshfree method with wavelet-based non-uniform nodes, where $N_{DI} = 2\times10^{17}\,\mathrm{cm}^{-3}$ is the doping of the active layer. It is significant to indicate that the Meshfree with uniform nodes gives precisely the same results as the conventional uniform FDTD method while the difference between the results of uniform and nonuniform cases is less than 1%. The final non-uniform grid and the

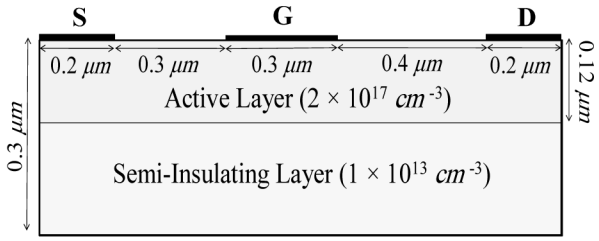

Fig. 1. The simulated MESFET structure.

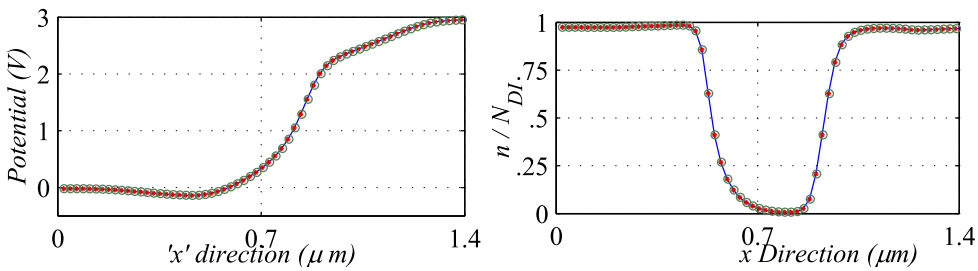

Fig. 2. Potential (left) and normalized carrier density (Right) across the 'x' direction at '$y = 0.09\,\mu$m'; '-': uniform FDTD, '*': uniform Meshfree, and 'o': wavelet-based non-uniform meshfree.

DOI: 10.1587/elex.8.1757
Received December 16, 2010
Accepted September 27, 2011
Published November 10, 2011

related $2D$ potential and the normalized carrier density distribution contour plot inside the transistor are shown in Fig. 3.

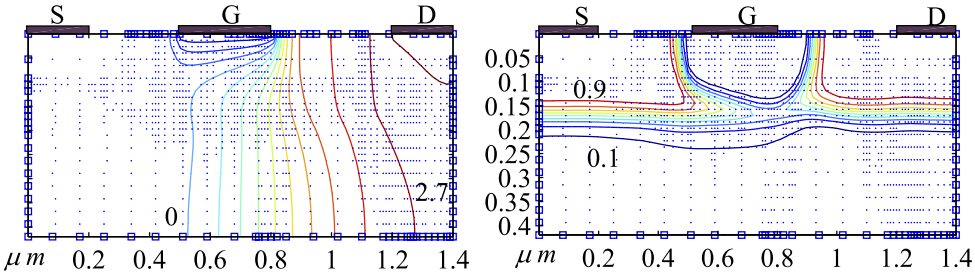

Fig. 3. Final non-uniform grid and contours of potential (left) and the normalized carrier density (Right) distribution.

5 Conclusion

This work proposed a numerical method for simulation of time dependent drift-diffusion model of semiconductor devices in two dimensions. The method is remarkably simple, especially for complicated domains and higher dimensions. Between radial basis functions a compactly supported version has been chosen due to the fact that it can result in a sparse matrix, and thus decrease the computational cost and memory requirements. The interpolating wavelet scheme was applied on DC simulation results to obtain an optimal sparse points representation for the nodes of meshless method. Large reduction in the number of nodes while the results remain acceptable leads to a large reduction of CPU time for the next AC simulation steps. Therefore, the presented method is suitable for the semiconductor part of very time consuming global modeling of microwave/millimeter wave circuits.

Acknowledgments

This work was supported in part by the Education & Research Institute for ICT.

DOI: 10.1587/elex.8.1757
Received December 16, 2010
Accepted September 27, 2011
Published November 10, 2011